PROCEEDINGS OF SCIENCE

Spectroscopy studies with $B \to DDX$ decays at LHCb

Raúl Iraq Rabadán Trejo[a,*] **on behalf of the LHCb collaboration**

[a] *The University of Warwick,*
Coventry CV4 7AL, United Kingdom

E-mail: raul.iraq.rabadan.trejo@cern.ch

The study of B-meson decays involving pairs of open-charm mesons presents significant opportunities for spectroscopy of excited open-charm and charmonium states, as well as the search for exotic states. This proceeding summarizes the latest amplitude analyses of $B \to DDX$ decays conducted by the LHCb collaboration.

42nd International Conference on High Energy Physics (ICHEP2024),
18-24 July 2024,
Prague, Czech Republic

*Speaker

https://pos.sissa.it/

PoS(ICHEP2024)440

1. $B \to DDX$ decays

The study of B-meson decays involving pairs of open-charm mesons provides excellent opportunities for spectroscopy of excited open-charm and charmonium states, as well as for searches for exotic states. Recent investigations into these decays have produced intriguing results. Notably, the LHCb collaboration has led efforts, including the first observation of tetraquark states in the D^-K^+ system through an amplitude analysis of $B^+ \to D^+D^-K^+$ decays [1, 2], and the first observation of a doubly charged charm tetraquark, along with its neutral partner, in the $B^+ \to D^-D_s^+\pi^+$ and $B^0 \to \overline{D}^0 D_s^+\pi^-$ decays [3, 4].

In this proceeding, a brief summary of LHCb's most recent amplitude analyses of $B \to DDX$ decays is presented. These analyses are based on proton-proton (pp) collision data collected with the LHCb detector at center-of-mass energies of 7 and 8 TeV (Run 1), and 13 TeV (Run 2), corresponding to a total integrated luminosity of approximately 9 fb^{-1}.

2. Amplitude analysis of $B^+ \to D^{*-}D_s^+\pi^+$ decays

The first amplitude analysis of the $B^+ \to D^{*-}D_s^+\pi^+$ decay is presented in [5]. Additionally, measurements of the branching fractions for the $B^+ \to D^{*-}D_s^+\pi^+$ and $B^+ \to D^{*-}D_s^{*+}\pi^+$ decays are reported, using the $B^0 \to D^{*-}D_s^+$ decay as a normalization channel.

Both decay chains, $B^+ \to D^{*-}D_s^+\pi^+$ and $B^0 \to D^{*-}D_s^+$, are reconstructed using the $\overline{D}^0 \to K^+\pi^-$ final state, with D^{*-} candidates formed from $\overline{D}^0\pi^-$ combinations. The D_s^+ candidates are reconstructed in the $K^+K^-\pi^+$ final state. To suppress combinatorial background, final state tracks are selected based on loose criteria for track-fit quality and kinematics. Additionally, D^0 and D_s^+ candidates are required to form good-quality vertices that are well separated from any primary vertices (PV). A boosted decision tree (BDT) is employed to further distinguish signal candidates from combinatorial background. Backgrounds resulting from misidentified final-state tracks are reduced by applying stricter particle identification criteria and vetoes.

The branching fraction of $B^+ \to D^{*-}D_s^+\pi^+$ is measured relative to $B^0 \to D^{*-}D_s^+$, with the ratio of branching fractions defined as $\mathcal{R} = \mathcal{B}(B^+ \to D^{*-}D_s^+\pi^+)/\mathcal{B}(B^0 \to D^{*-}D_s^+)$. The yields for both the signal and normalization decays are extracted by fitting the $D^{*-}D_s^+\pi^+$ and $D^{*-}D_s^+$ invariant mass distributions. Contributions from partially reconstructed B meson decays appear in the region below the B meson mass peak, originating from B meson decays where the D_s^{*+} decays as $D_s^{*+} \to D_s^+\gamma/\pi^0$, with the photon or π^0 not being reconstructed. The analysis also measures the ratio of the branching fractions for $B^+ \to D^{*-}D_s^{*+}\pi^+$ and $B^+ \to D^{*-}D_s^+\pi^+$, denoted as $\mathcal{R}^*$. The ratios of branching fractions obtained from the fit are $\mathcal{R} = 0.173 \pm 0.006 \pm 0.010$ and $\mathcal{R}^* = 1.32 \pm 0.07 \pm 0.14$, where the first uncertainty is statistical and the second is systematic.

The invariant mass distributions for the $D^{*-}D_s^+$ and $D^{*-}D_s^+\pi^+$ combinations, along with the fit results, are shown in Fig. 1. For the $B^+ \to D^{*-}D_s^+\pi^+$ mode, only candidates within the $|m(D^{*-}D_s^+\pi^+) - m_{B^+}| < 30$ MeV window are selected for the amplitude fit.

Various amplitude models are employed to fit the data. The baseline fit exclusively incorporates resonance activity in the $D^{*-}\pi^+$ channel. The parametrisation of excited charm-meson resonances decaying to the $D^{*-}\pi^+$ final state employs Breit–Wigner line shapes. The invariant-mass projections of the baseline fit result are presented in Fig. 2. The analysis reveals that the amplitude is dominated

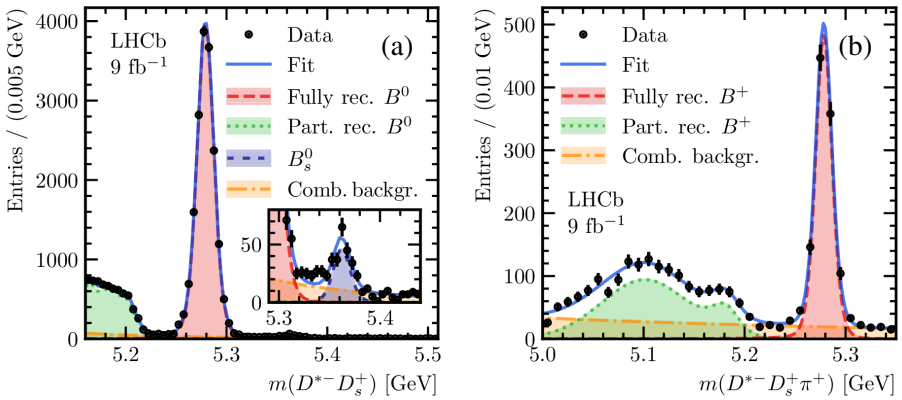

Figure 1: Invariant-mass distributions of (a) $D^{*-}D_s^+$ and (b) $D^{*-}D_s^+\pi^+$ combinations and the results of the fits used to obtain the yields of the $B^0 \to D^{*-}D_s^+$, $B^+ \to D^{*-}D_s^+\pi^+$ and $B^+ \to D^{*-}D_s^{*+}\pi^+$ decays. The inset in the plot (a) shows a zoomed region with the contribution of the $B_s^0 \to D^{*-}D_s^+$ decay component.

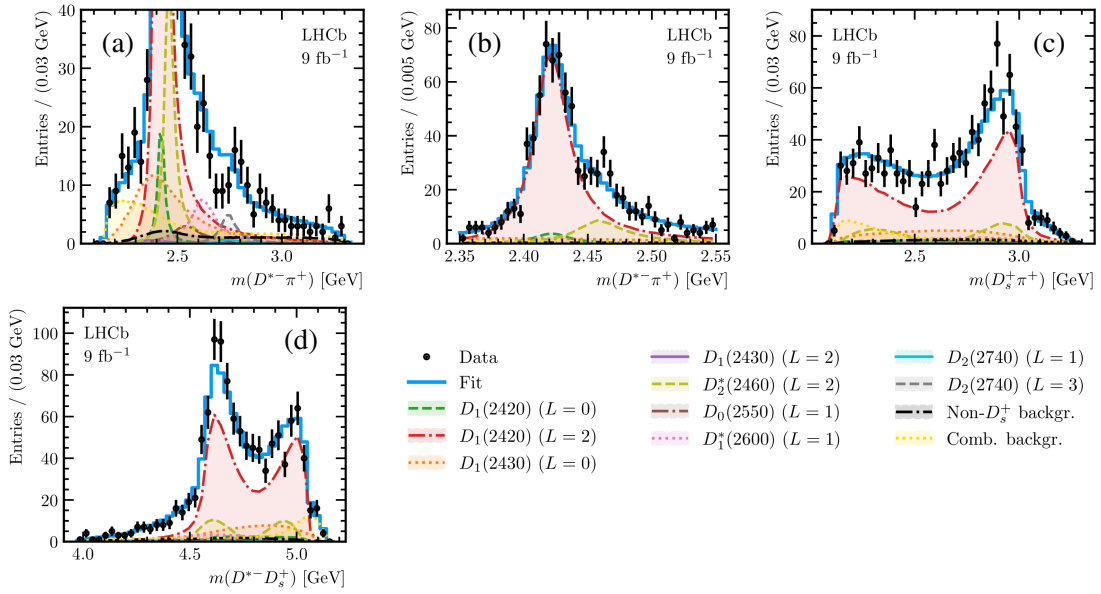

Figure 2: Results of the fit of the $B^+ \to D^{*-}D_s^+\pi^+$ distribution with the baseline model. Figures (a) and (b) show the $m(D^{*-}\pi^+)$ projection, with (a) zoomed in to illustrate the contributions from all the resonances while (b) shows the projection near the $D_1(2420)$ resonance. The $m(D_s^+\pi^+)$, $m(D^{*-}D_s^+)$, projections are shown in (c), (d), respectively.

by the following resonances in the $D^{*-}\pi^+$ channel: $D_1(2420)$, $D_1(2430)$, $D_2^*(2460)$, $D_0(2550)$, $D_1^*(2600)$, $D_2(2740)$. The fit fractions and phases for these components are extracted and reported in [5].

Alternative fits exploring potential exotic contributions in the $D_s^+\pi^+$ and $D^{*-}D_s^+$ channels are also examined. However, no significant evidence of exotic contributions is observed in either the $D^{*-}D_s^+$ or $D_s^+\pi^+$ channels. The fit fraction of the scalar state $T^*_{c\bar{s}0}(2900)^{++}$ in the $D_s^+\pi^+$ channel observed in the $B^+ \to D^-D_s^+\pi^+$ analysis [3, 4] is found to be less than 2.3% at 90% CL.

3. Observation of new charmonium(-like) states in $B^+ \to D^{*\pm}D^{\mp}K^+$ decays

A study of the resonant composition in the decays $B^+ \to D^{*+}D^-K^+$ and $B^+ \to D^{*-}D^+K^+$ is presented in [6]. A simultaneous amplitude fit is performed to the two channels, exploiting the C-parity relation between contributions from charmonium(-like) resonances decaying to $D^{*+}D^-$ and $D^{*-}D^+$ final states.

The decay channels $B^+ \to D^{*+}D^-K^+$ and $B^+ \to D^{*-}D^+K^+$ are reconstructed using $D^{*-} \to \overline{D}^0\pi^-$, $\overline{D}^0 \to K^+\pi^-$, $\overline{D}^0 \to K^+\pi^-\pi^-\pi^+$, and $D^- \to K^+\pi^-\pi$ final states. Preselection criteria select high-quality tracks displaced from the PV, with charmed and B meson candidates required to have high-quality vertices and be well displaced from any PV. A BDT classifier reduces combinatorial backgrounds using topological and PID information. Backgrounds with one or no charmed mesons are further suppressed by requiring significant flight distances for the reconstructed D meson candidates from the B^+ decay vertex. After selection, 1636 ± 43 and 1772 ± 44 signal decays are available for the amplitude fit in the $B^+ \to D^{*+}D^-K^+$ and $B^+ \to D^{*-}D^+K^+$ channels, respectively.

The amplitude model is constructed to allow for resonant activity in various two-body channels. Due to C-parity conservation in strong decays, any charmonium(-like) resonance R contributes equally to $B^+ \to R(D^{*+}D^-)K^+$ and $B^+ \to R(D^{*-}D^+)K^+$, linking their amplitudes through C-parity in the simultaneous fit. However, interference between resonances with different C-parities can result in differences between the two final states, which can be used to determine the C-parities of the R resonances. No such constraints are applied to resonances decaying to $D^{*\mp}K^+$ or $D^{\pm}K^+$.

The lineshapes used to parametrize $R \to D^{*\pm}D^{\mp}$ resonances with $J^P = 1^+$ are given by

$$f_{R,S/D}(m) = \frac{\gamma_{S/D}}{m_0^2 - m^2 - im_0[\gamma_S^2\Gamma_S(m) + \gamma_D^2\Gamma_D(m)]},$$

where $\gamma_{S(D)}$ denote the S-wave (D-wave) coupling constants, determined from the fit and satisfying the constraint $\gamma_S^2 + \gamma_D^2 = 1$, m represents the reconstructed mass, m_0 is the pole mass, and $\Gamma(m)$ the mass-dependent width. Other resonances are described using Breit–Wigner lineshapes.

The baseline model incorporates resonant activity in the $D^{*\pm}D^{\mp}$ and D^-K^+ channels. The invariant mass projections from the baseline fit are compared to the data in Fig. 3. The model includes contributions from the $\chi_{c2}(3930)$ and $\psi(4040)$, with their mass parameters fixed to known values. At the $D^{*\pm}D^{\mp}$ threshold, a 1^{++} contribution is required to describe the mass distributions, and the tail of the $\chi_{c1}(3872)$ is used as an effective model. Four additional nonresonant (NR) components are needed to describe the $D^{*\pm}D^{\mp}$ mass spectrum, with their line shapes set to $f_R = 1$, except for the $J^P = 0^{-+}$ component, which is modeled by an exponential NR shape with parameters determined from the fit.

The inclusion of the two resonant contributions, $T^*_{\bar{c}\bar{s}0}(2870)^0$ and $T^*_{\bar{c}\bar{s}1}(2900)^0$, previously found in the $B^+ \to D^+D^-K^+$ decay, successfully describes the enhancement observed in the D^-K^+ mass distribution. The statistical significances of $T^*_{\bar{c}\bar{s}0}(2870)^0$ and $T^*_{\bar{c}\bar{s}1}(2900)^0$ are 11σ and 9.2σ, respectively, confirming their existence in this new decay mode.

Additionally, four charmonium-like states, identified as $\eta_c(3945)$, $h_c(4000)$, $\chi_c(4010)$, and $h_c(4300)$, are included to describe the spectrum. Their quantum numbers J^{PC} are determined to be 0^{-+}, 1^{+-}, 1^{++}, and 1^{+-}, respectively, with corresponding statistical significances of 10σ, 9.1σ, 16σ, and 6.4σ. The resonance parameters extracted from the fit are reported in [6].

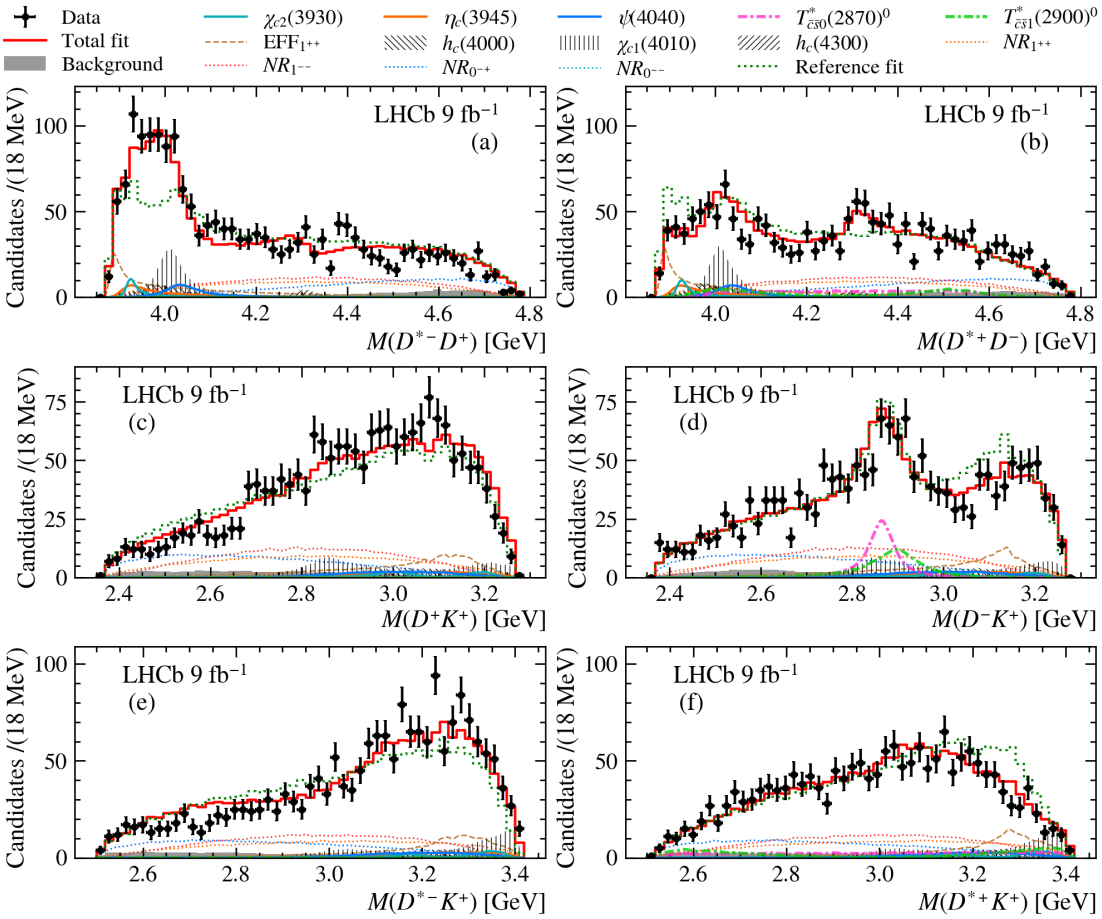

Figure 3: Distributions of two-body invariant masses: (a) $M(D^{*-}D^+)$, (c) $M(D^+K^+)$ and (e) $M(D^{*-}K^+)$ in the $B^+ \to D^{*-}D^+K^+$ sample; (b) $M(D^{*+}D^-)$, (d) $M(D^-K^+)$ and (e) $M(D^{*+}K^+)$ in the $B^+ \to D^{*+}D^-K^+$ sample. The fit results (red-solid lines) are over- laid on the data distributions. Contributions from different components are also shown in different line styles as indicated in the legend. The result of fitting the data using a model without the $h_c(4000)$, $\chi_c(4010)$ and $h_c(4300)$ components (reference fit) is shown with green-dotted lines for comparison

4. Conclusions and future prospects

The investigation of $B \to DDX$ decays remains an active field within the LHCb collaboration, with more results still expected from the full analysis of the Run 1 and Run 2 datasets. These analyses are expected to yield new discoveries and contribute to improve the understanding of hadronic interactions and the nature of exotic states.

Looking ahead for the upcoming data from the LHC Run 3, the upgraded LHCb detector will significantly boost the efficiency of fully hadronic decay analyses, particularly due to the removal of the hardware trigger. This improvement will enable more spectroscopy studies. The increased luminosity and improved detector performance will allow LHCb to explore more complex decay modes and search for new resonances, further advancing the field of heavy-flavor physics and hadron spectroscopy in the coming years.

References

[1] LHCb Collaboration collaboration, *Model-independent study of structure in $B^+ \to D^+D^-K^+$ decays*, *Phys. Rev. Lett.* **125** (2020) 242001.

[2] LHCb Collaboration collaboration, *Amplitude analysis of the $B^+ \to D^+D^-K^+$ decay*, *Phys. Rev. D* **102** (2020) 112003.

[3] LHCb Collaboration collaboration, *First observation of a doubly charged tetraquark and its neutral partner*, *Phys. Rev. Lett.* **131** (2023) 041902.

[4] LHCb Collaboration collaboration, *Amplitude analysis of $B^0 \to \overline{D}^0 D_s^+\pi^-$ and $B^+ \to D^-D_s^+\pi^+$ decays*, *Phys. Rev. D* **108** (2023) 012017.

[5] LHCb collaboration, *Amplitude analysis and branching fraction measurement of $B^+ \to D^{*-}D_s^+\pi^+$ decays*, *JHEP* **08** (2024) 165.

[6] LHCb collaboration collaboration, *Observation of new charmonium(-like) states in $B^+ \to D^{*\pm}D^{\mp}K^+$ decays*, LHCb-PAPER-2023-047.